


Exploring the Potential of Chaihu-Danggui Tang in Breast Cancer Treatment Based on Network Pharmacology, Molecular Docking, and Experimental Validation

Yusheng Liu^{1,2,*}, Junfeng Zhang^{3,*}, Yigui Lai¹, Chunying Wu¹, Dongsheng Liu², Rongyao Liang¹, Gang Chen¹, Xuefeng Jiang^{1,2} 

¹Comprehensive Laboratory, Yangjiang People's Hospital, Yangjiang, 529500, People's Republic of China; ²Department of Traditional Chinese Medicine, Hainan West Central Hospital, Danzhou, 571700, People's Republic of China; ³School of Medicine, Anhui University of Science and Technology, Huainan, 232001, People's Republic of China

*These authors contributed equally to this work

Correspondence: Xuefeng Jiang; Gang Chen, Email 670621447@qq.com; xy7224@163.com

Background: Chaihu-Danggui Tang (CHDGT) has a long history in traditional Chinese medicine (TCM) as an adjuvant therapy for breast cancer (BC), but its precise anti-tumor mechanisms remain unknown. In this study, we used network pharmacology, molecular docking, and experimental validation methods to investigate the core components, key targets, and possible mechanisms through which CHDGT may exert therapeutic effects in BC treatment.

Methods: The Traditional Chinese Medicine Systems Pharmacology (TCMSP) was employed to obtain the active ingredient and targets of CHDGT. Meanwhile, the GeneCards databases were used to retrieve pertinent targets for BC. The Venn plot was used to obtain intersection targets. Cytoscape software was used to construct an “CHDGT-active ingredients-targets” network and identify core targets. The common targets after STRING processing were imported into the Metascape database for GO and KEGG pathway enrichment analysis. Molecular docking of key ingredients and core targets of drugs was accomplished using Autodock and PyMol software. The cell and animal experiments confirmed CHDGT efficacy and mechanism in treating BC.

Results: We screened 5 key effector components, 8 core targets, and multiple signaling pathways of CHDGT in treating BC. In vitro, the results of CCK-8 assay showed that CHDGT can dose-dependently inhibits BC cell growth, and at 100 mg L⁻¹ after 48 hours, the cell inhibition rate reached approximately 50%. Further analysis showed that CHDGT can promote apoptosis of BC cell, and regulate the expression levels of apoptosis-related genes, such as Caspase3, p53, and Bcl-2. The animal experiments verified that CHDGT can significantly inhibit the progression of BC, the tumor inhibition rate of CHDGT-H groups was as high as 60.06 ± 4.82%. In addition, H&E staining and blood biochemical analysis suggest that CHDGT exhibits favorable safety.

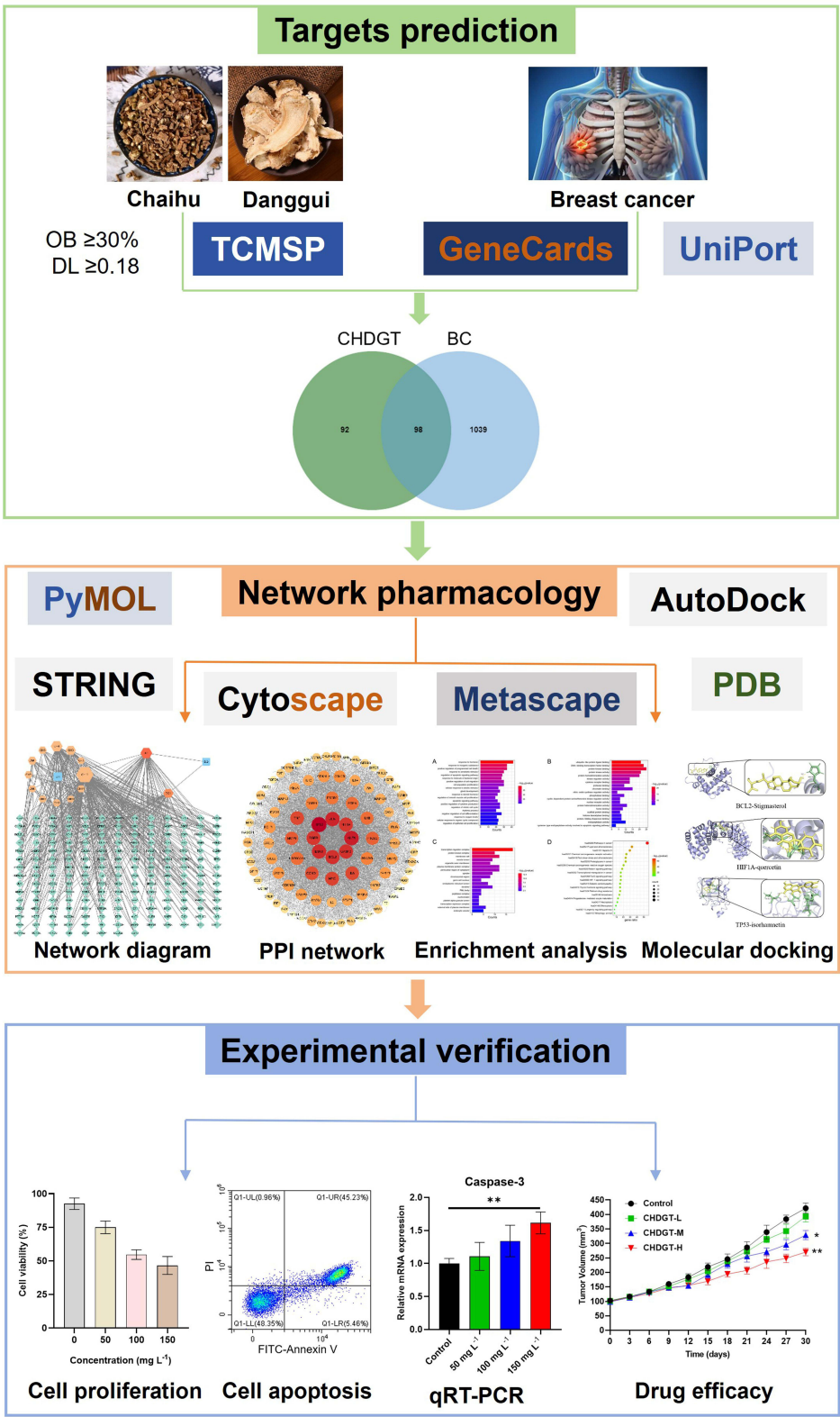
Conclusion: This study may provide perspectives for the development of anticancer Chinese herbs for the treatment of BC.

Keywords: chaihu-danggui tang, breast cancer, network pharmacology, molecular docking, apoptosis

Introduction

According to the 2024 report by the World Health Organization (WHO), there were 19.96 million new cancer cases globally in 2022, with breast cancer (BC) ranking second, and estimates that by 2040, BC cases are projected to exceed 3 million, with over 1 million deaths expected.¹ Current breast cancer management primarily involves surgical intervention tailored to the disease stage, often supplemented by radiotherapy, chemotherapy, immunotherapy, or targeted therapy.^{2,3} While these approaches have significantly enhanced survival rates, they can impose substantial financial burdens and adversely affect patients' life. Consequently, there is a pressing need to explore cost-effective and low-toxicity therapeutic options. Traditional Chinese Medicine (TCM) is frequently recognized for its milder side effects

Graphical Abstract



compared to conventional treatments, offering potential benefits in reducing treatment-related discomfort. Emphasizing evidence-based approaches, TCM adopts a holistic strategy that not only targets tumor eradication but also supports immune modulation and overall patient constitution, aiming to enhance recovery and improve quality of life.⁴

Chaihu is a widely used Chinese herb, known for its ability to reduce fever, elevate yang qi, soothe the liver, and alleviate depression. Additionally, it exhibits anti-inflammatory, neuromodulatory, antiviral, and anti-tumor properties.⁵ Danggui, another herb in TCM, has been used for millennia, first documented in the “Shennong Bencaojing” for its functions in nourishing and promoting blood circulation, alleviating pain, and lubricating the intestines.⁶ Modern pharmacological research shows that Danggui has the effect of treating anemia, protecting liver and anti-tumor.⁷ The Chaihu-Danggui is a commonly prescribed combination in TCM. However, its multi-component and multi-target characteristics create challenges in understanding its molecular mechanisms, highlighting the gap between foundational research and therapeutic application. Addressing these complexities is critical for advancing TCM development.

Network pharmacology combining bioinformatics and pharmacology methods, offers a systematic framework to explore the intricate “disease-gene-target-drug” interactions, thereby providing new insights into the mechanisms of TCM.⁸ On the other hand, molecular docking is a theoretical simulation method that mainly studies the interaction between molecules (such as ligands and receptors) and predicts their binding patterns and affinity.⁹ In recent years, molecular docking has become an important technology in the field of computer-aided drug research.

In this study, we integrated network pharmacology, molecular docking, and experimental validation to investigate the active components, potential targets, and potential mechanisms of Chaihu-Danggui Tang (CHDGT) in breast cancer treatment.

Materials and Methods

Network Pharmacological Analysis

Analysis of Active Chemical Ingredients and Targets in CHDGT

The Chinese Medicine System Pharmacological (TCMSP) database (<https://tcmspw.com/tcmsp.php>) was used to screen the chemical ingredients of Chaihu and Danggui, according to oral bioavailability (OB) $\geq 30\%$ and drug-likeness (DL) ≥ 0.18 .¹⁰ In addition, we searched the relevant literature in the Web of Science database to add other major chemical ingredients. The target proteins corresponding to each component were obtained from the TCMSP database, and then these target proteins were transformed into human species genes through the UniProt database.

The “CHDGT-Active Ingredients-Targets” Network

Based on the interaction of drugs, ingredients and gene symbols, the “CHDGT-active ingredients-targets” network was constructed using Cytoscape 3.10.2.

Collection of BC Target Genes

Using “breast cancer” as a keyword, BC-related genes were searched in GeneCards database (<https://www.genecards.org/>), according to the median principle to select target. Then, we used Venny 2.1.0 (<http://www.bioinformatics.com.cn/>) to intersect the targets of CHDGT ingredients and BC-related targets. The overlapping genes were thought to targets of CHDGT active ingredients for the treatment of BC and were visualized by using Venn diagram.

Analysis of Protein–Protein Interaction

The PPI network of intersecting targets of CHDGT and BC was constructed using STRING database (<https://string-db.org/>) and Cytoscape 3.10.2 software.

Gene Ontology Analysis and KEGG Pathway Enrichment Analysis

The common targets after STRING processing were imported into the Metascape database (<https://metascape.org/>) for GO analysis and KEGG pathway enrichment analysis. GO analysis includes cellular component (CC), molecular function (MF), and biological process (BP). KEGG (<https://www.genome.jp/kegg/>) enrichment focuses on biological pathways associated with target genes. Use the bioinformatics mapping website (<http://www.bioinformatics.com.cn/>) to plot bar charts and bubble charts for the top 20 GO terms and the top 20 KEGG pathways with the lowest P values.

Molecular Docking

Download the 3D structure PDB ID of the target protein from the PDB database (<https://www.pdb.org/>). Target protein containing the original ligand, after the original ligand is removed, is attached to the binding pocket of the protein. Root mean square deviation (RMSD) between the accordance of the docked ligand and the primary crystalline structure was computed. It is commonly supposed that the composite target interaction way is credible if $\text{RMSD} \leq 2 \text{ \AA}$.

The 5 key components with the most targets in “CHDGT-active ingredients-interactive targets” network were selected, and the three-dimensional (3D) structure search was searched for these compounds using the PDB database. The targets with the top 8 degree value was selected in the drug-disease common target PPI network. Autodock software was used for molecular docking simulation and PyMol 3.0.4 was used for visualization.

Experimental Validation

Preparation of CHDGT Extract

CHDGT is composed of Chaihu (*Bupleurum chinense* DC). and Danggui (*Angelica sinensis* (Oliv). Diels). Chaihu (Batch No.: 230301) and Danggui (Batch No.: 230203) in this study were purchased from Nanfang Hospital (Guangzhou, China). The samples were kept at the comprehensive laboratory of Yangjiang People's Hospital. All plant names have been verified using <http://www.theplantlist.org> and adhere to plant nomenclature standards.

Preparation method: 500 g each of Chaihu and Danggui were weighed, the herbs (the mass ratio of Chaihu and Danggui was 1:1) were soaked in 8 times the amount of pure water for 1 h, boiled for 50 minutes, then pour out the liquid, and then added 5 times the amount of water to boil directly, and pour out the liquid after 40 minutes. The liquid from the above two pours was mixed and filtered with gauze, and the supernatant was concentrated to 500 mL with a rotary evaporator. And the supernatant was frozen overnight at -80°C and freeze-dried to obtain 32.5 g freeze-dried powder. In in vitro experiments, we dissolved CHDGT powder in the required concentration of culture medium. In animal experiments, CHDGT was administered orally to mice.

Cell Culture and Treatment

4T1 cells (mouse breast cancer cell line) was purchased from the Chinese Academy of Sciences. Cells were maintained in a culture medium of DMEM supplementing with 10% FBS and incubated at 37°C and 5% CO_2 . CHDGT freeze-dried powder was dissolved in the medium and diluted to different concentrations (0, 50, 100, 150 mg L^{-1}), and incubated the cells for 24 h, 48 h, and 72 h, respectively. The other experimental groups were control group, CHDGT group (100 mg L^{-1}), HIF-1 α activator group (100 μM), CHDGT plus HIF-1 α activator group. The cells in each group were incubated at 37°C for 48 h.

Cell Counting Kit-8 (CCK-8) Assay

4T1 cells were inoculated into 96-well plates (5×10^3 cells per well), and treatment with different concentrations of CHDGT (0, 50, 100, 150 mg L^{-1}) for 24, 48, 72 h, and with CHDGT (100 mg L^{-1}) and Dimethyloxallyl Glycine (DMOG, HIF-1 α activator, 100 μM) group for 48 h, 10 μL CCK-8 solution (Dojindo Laboratories, Japan) was added to each well. After incubation at 37°C for 1 h, the absorbance of each well at 450 nm was measured.

Cell Apoptosis

Annexin V-FITC/PI Apoptosis Detection Kit (BD, USA) was used to analyze cell apoptosis. The 4T1 cells were inoculated into 6-well plates (1×10^6 cells per well) and cultured in CO_2 incubator for 24 h. After culturing 4T1 cells with CHDGT solution (100 mg L^{-1}) for 48 h, the cells were processed according to the protocol of Annexin V-FITC/PI Apoptosis Detection Kit (BD, USA) and analyzed by flow cytometry. Each experiment was performed in triplicate.

Quantitative Real-Time PCR

The expression levels of Caspase-3, Bcl-2, p53, and HIF-1 α genes were quantified using qRT-PCR. Total RNA was extracted from 4T1 cells with Trizol reagent (Invitrogen, USA) following the manufacturer's protocol. First-strand cDNA was synthesized from 2 μL of RNA using the RevertAid First Strand cDNA Synthesis Kit. PCR reactions were performed in triplicate using 25 μL of reverse transcription product, with an initial denaturation at 95°C for 10 minutes,

followed by 40 cycles of 95°C for 15 seconds and 60°C for 1 minutes. A melting curve analysis was conducted from 75°C to 95°C, increasing by 1°C every 20 seconds.

Therapeutic Effect in vivo

The female BALB/c mice used in the experiment were purchased from the Shanghai Laboratory Animal Center (Shanghai, China). 4T1 cell suspension (1×10^7 cells/100 μ L) were subcutaneously injected into the right side of the mouse. The mice were randomly divided into 4 groups with 6 mice in each group, when the tumor volume reached approximately 100 mm³: control group (normal saline), CHDGT low-dose group (CHDGT-L, 3.5 g/kg), CHDGT medium-dose group (CHDGT-M, 7 g/kg), CHDGT high-dose group (CHDGT-H, 14 g/kg). Tumor size and body weight of mice were measured every three days after treatment. Tumor volume was determined according to the following formula: $V = LW^2/2$ (L: tumor length, W: tumor width). Each group of mice were treated for 30 days. At the end of the experiment, all mice were sacrificed. The tumor tissues of each group of mice were taken and weighed. The main organs (heart, liver, spleen, lung, and kidney) were fixed with 4% paraformaldehyde. All animal experiments were performed following “the National Regulation of China for Care and Use of Laboratory Animals” and were approved by the Institutional Animal Care and Use Committee of Anhui University of Science and Technology (approval number, S22024014).

Evaluation of Toxicity in vivo

After the end of the experiment, blood samples of mice were collected, and serum was obtained by centrifugation at 3000 rpm for 5 min. Liver function was evaluated by assessing the serum levels of ALT, AST, ALP, and LDH. UREA and CRE levels were assessed to evaluate nephrotoxicity. Blood biochemical tests were performed according to commercial kit instructions (Beyotime, Shanghai, China).

Hematoxylin and Eosin (H&E) Staining

The tissues were fixed with 4% (v v⁻¹) paraformaldehyde, embedded in a paraffin block, sectioned into 5 μ m thickness, and then placed onto glass slides. After staining with H&E, the slides were examined by a pathologist using an optical microscope.

Statistical Analysis

Statistical analysis was analyzed using GraphPad Prism 8.0. Differences between the two groups were measured by *T*-test, and comparisons between the groups were evaluated by one-way analysis of variance (ANOVA). The data were expressed as mean \pm SEM. **P* < 0.05, ***P* < 0.01, ****P* < 0.001 were considered significant.

Results

Network Pharmacological Analysis

Active Ingredients and Targets of CHDGT in the Treatment of BC

We collected the active ingredients of each herb in CHDGT (OB \geq 30% and DL \geq 0.18) from the TCMSP database. We identified 17 active ingredients of Chaihu, only 2 components of Danggui were identified under the same criteria. To enhance the analysis, 3 additional components were supplemented from the literature. The stigmasterol exists both in Chaihu and Danggui ([Supplementary Tables S1–S3](#)). Target proteins corresponding to the active ingredients were retrieved from the TCMSP database, and their gene names were standardized via the UniProt database. After excluding 8 ingredients without target information, 14 active compounds of CHDGT were selected for further analysis ([Table 1](#)). Duplicate targets associated with different ingredients were consolidated, yielding a total of 190 unique gene targets ([Supplementary Table S4](#)). In addition, we constructed a “CHDGT-active ingredients-targets” network using Cytoscape 3.7.2 ([Figure 1A](#)). The top 5 active ingredients included quercetin, stigmasterol, kaempferol, beta-sitosterol, and isorhamnetin.

With the use of “breast cancer” as the search term, 1137 BC-related genes were obtained from the GeneCards database, according to the median principle to select target ([Supplementary Table S5](#)). We compared the obtained 190

Table I Main Active Chemical Ingredients of CHDGT

ID	MOL ID	Active Ingredients	OB (%)	DL	Source
CH1	MOL001645	Linoleyl acetate	42.1	0.19	Chai Hu
CH2	MOL002776	Baicalin	40.12	0.75	Chai Hu
CH3	MOL000354	isorhamnetin	49.6	0.3	Chai Hu
CH4	MOL000422	kaempferol	41.88	0.24	Chai Hu
CH5	MOL004598	3,5,6,7-tetramethoxy-2-(3,4,5-trimethoxyphenyl) chromone	31.97	0.59	Chai Hu
CH6	MOL004609	Areapillin	48.96	0.41	Chai Hu
CH7	MOL013187	Cubebin	57.12	0.63	Chai Hu
CH8	MOL004624	Longikaurin A	47.72	0.53	Chai Hu
CH9	MOL004653	(+)-Anomalin	46.05	0.65	Chai Hu
CH10	MOL004718	α -spinasterol	42.97	0.75	Chai Hu
CH11	MOL000490	petunidin	30.04	0.3	Chai Hu
CH12	MOL000098	quercetin	46.43	0.27	Chai Hu
A1	MOL000449	Stigmasterol	43.82	0.75	Chai Hu, Dang Gui
DG1	MOL000358	Beta-sitosterol	36.91	0.75	Dang Gui

drug targets with 1137 BC-related genes, obtaining 98 overlapping genes that may be the most key genes for CHDGT-related treatment of BC (Figure 1B and Supplementary Table S6).

The PPI Network of Intersecting Targets of CHDGT and BC

The PPI network was constructed for the 98 overlapping genes identified as potential key targets of CHDGT in BC treatment using the STRING database. The resulting network comprised 98 nodes and 2373 edges (Supplementary Figure S1). Node degree, representing the number of interactions for each gene, was used to identify critical genes. The

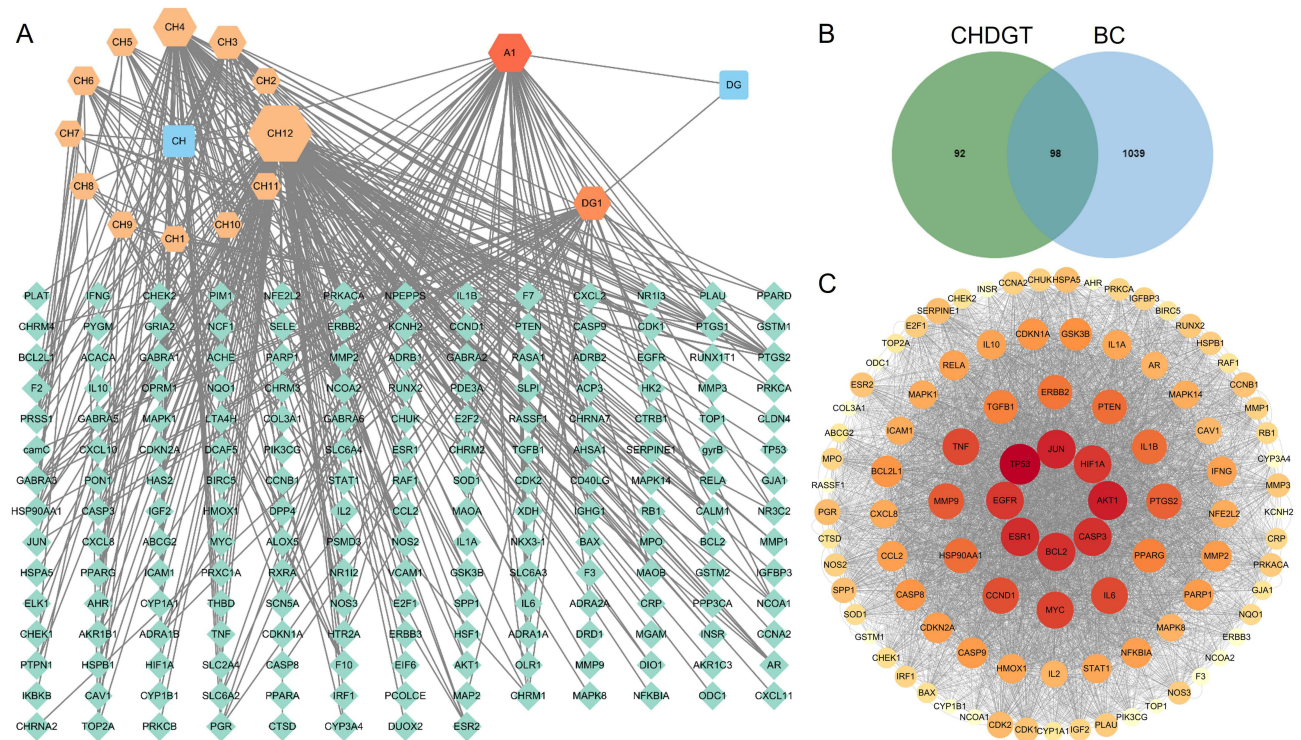


Figure 1 Network pharmacological study of CHDGT for BC. (A) Network diagram of “CHDGT-active ingredients-targets”. (B) Venn diagram of CHDGT-BC interaction targets. (C) The PPI network of intersecting targets of CHDGT and BC.

node degree average of the 98 overlapping genes was 48.4, and the average local clustering coefficient was 0.766. Arranged by degree values, a network of interactions between proteins were constructed by Cytoscape (Figure 1C).

The inner loop shows the core 8 genes (TP53, AKT1, JUN, ESR1, BCL2, CASP3, HIF1A, and EGFR) with higher degree values. [Supplementary Table S7](#) provides detailed information on these genes and their topological properties.

GO and KEGG Pathway Enrichment Analysis

To reveal the roles of CHDGT in treating BC, we performed GO and KEGG enrichment analyses on the 98 overlapping genes ($P < 0.01$). The top 20 enriched terms in the molecular function (MF), biological process (BP), and cellular component (CC) categories were identified. The results showed that the main BP terms included response to hormone, regulation of apoptotic signaling pathway, positive regulation of cell migration, and cell population proliferation (Figure 2A). The main MF terms included ubiquitin-like protein ligase binding, protein kinase binding, kinase regulator activity, and cytokine receptor binding (Figure 2B). The main CC terms included protein kinase complex, membrane raft, vesicle lumen, and organelle outer membrane (Figure 2C).

For pathway analysis, KEGG enrichment identified 20 significantly enriched signaling pathways ($P < 0.01$), visualized based on count and p-value metrics (Figure 2D). The results showed that the targets were mainly enriched in pathways such as pathways in cancer, chemical carcinogenesis-reactive oxygen species, HIF-1 signaling pathway, FoxO signaling pathway, and necroptosis.

Molecular Docking

Five core ingredients (quercetin, stigmasterol, kaempferol, isorhamnetin, and beta-sitosterol) and top 8 core targets (TP53, AKT1, JUN, ESR1, BCL2, CASP3, HIF1A, and EGFR) to assess the protein-ligand binding potential by

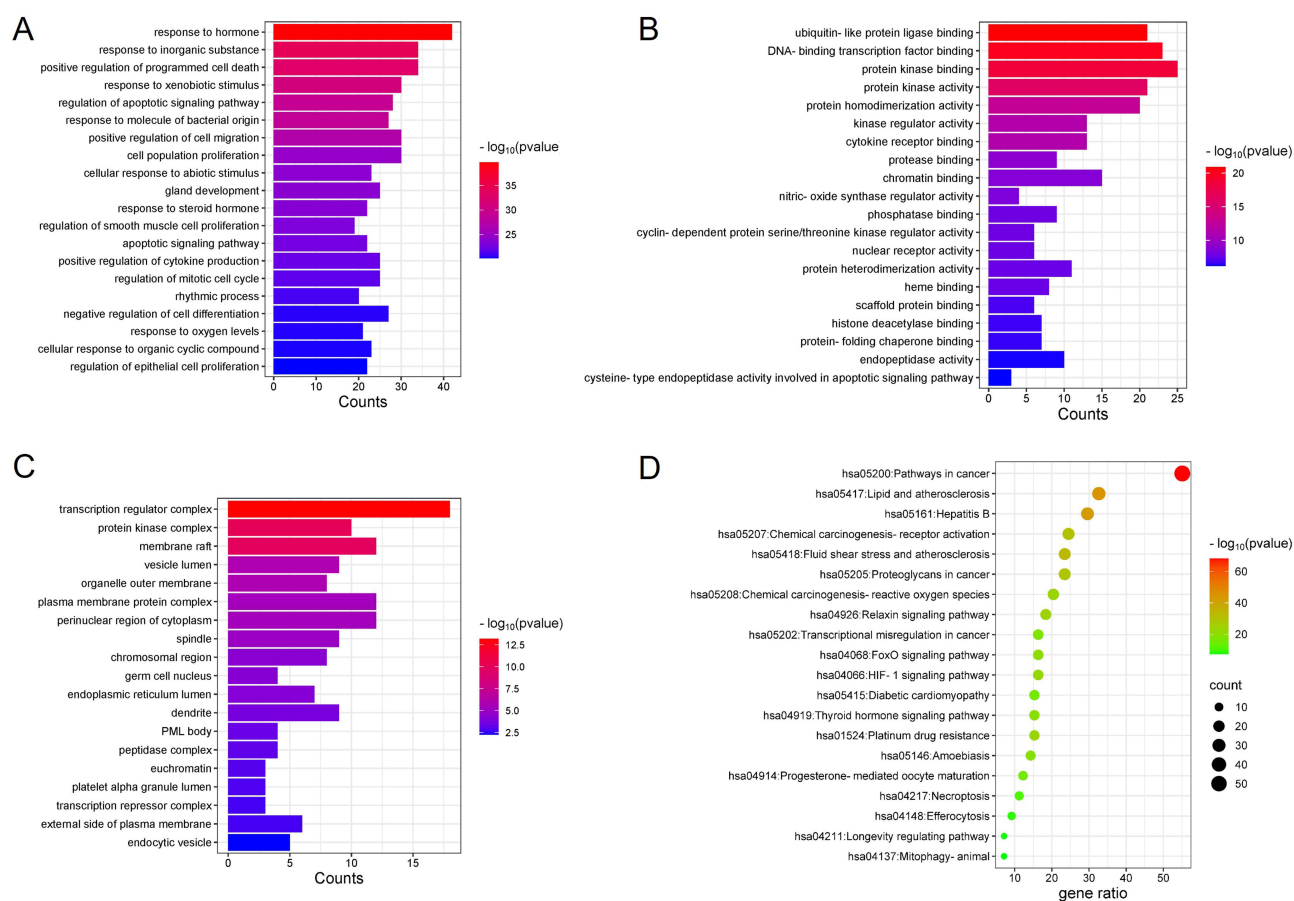


Figure 2 (A–C) GO enrichment analysis results in biological processes (BP), molecular functions (MF), and cellular ingredients (CC). **(D)** KEGG pathway enrichment analysis.

molecular docking. Affinity measures the strength of binding between a ligand and its receptor, with a more negative binding energy indicating stronger interactions.

Molecular docking analysis revealed that five active ingredients of CHDGT displayed robust binding affinity to their respective targets, the binding energies were almost all below -4 kcal/mol, and the majority of RMSD were less than 2.0 Å (Table 2). These findings confirm the therapeutic potential of CHDGT in BC treatment at the molecular docking level. The top 10 ligand-target complexes, ranked by absolute binding affinity, were HIF1A-kaempferol, BCL2-stigmasterol, BCL2-quercetin, HIF1A-quercetin, HIF1A-stigmasterol, TP53-isorhamnetin, AKT1-isorhamnetin, JUN-kaempferol, CASP3-isorhamnetin, and EGFR-beta-sitosterol. The docking results as follows: HIF1A was docked to kaempferol with four hydrogen bonds, including GLN-329 (3.4 Å), THR-328 (3.0 Å), THR-324 (2.7 Å) and ASP-368 (2.3 Å). BCL2

Table 2 Target Proteins Docking Results for Compounds

Protein (PDB ID)	Compound	Binding Energy (kcal/mol)	RMSD
TP53 (3D06)	quercetin	-4.26	2.4175
	Stigmasterol	-4.16	1.9599
	kaempferol	-4.31	1.8077
	isorhamnetin	-6.05	0.8701
	beta-sitosterol	-4.66	1.6881
AKT1 (1UNP)	quercetin	-4.72	1.8795
	Stigmasterol	-4.05	2.9042
	kaempferol	-4.71	1.2655
	isorhamnetin	-5.90	0.8979
	beta-sitosterol	-4.28	2.1967
JUN (5T01)	quercetin	-4.33	2.2481
	Stigmasterol	-4.68	1.8093
	kaempferol	-5.84	0.9086
	isorhamnetin	-3.80	2.3508
	beta-sitosterol	-4.20	2.1477
ESR1 (3OS8)	quercetin	-5.26	1.9813
	Stigmasterol	-4.13	2.9007
	kaempferol	-4.21	2.5438
	isorhamnetin	-4.97	1.5990
	beta-sitosterol	-4.96	2.5803
BCL2 (1G5M)	quercetin	-6.55	0.6825
	Stigmasterol	-6.82	0.4280
	kaempferol	-5.33	1.5182
	isorhamnetin	-3.50	2.4711
	beta-sitosterol	-4.80	1.7263
CASP3 (3H0E)	quercetin	-4.74	1.5893
	Stigmasterol	-4.49	1.2994
	kaempferol	-5.71	1.1843
	isorhamnetin	-5.88	0.9672
	beta-sitosterol	-4.20	2.2749
HIF1A (8HE0)	quercetin	-6.28	0.7067
	Stigmasterol	-6.22	0.8210
	kaempferol	-7.27	0.1783
	isorhamnetin	-3.25	2.6619
	beta-sitosterol	-4.11	2.5691
EGFR (3W33)	quercetin	-4.88	1.386
	Stigmasterol	-4.03	1.5395
	kaempferol	-5.33	1.1904
	isorhamnetin	-4.97	1.9935
	Beta-sitosterol	-5.74	0.9981

could bind to stigmasterol by hydrogen bond with HIS-20 (2.0Å). BCL2 was docked to quercetin with four hydrogen bonds, including HIS-94 (2.6Å), TYR-18 (2.5Å), TYR-9 (1.8Å) and ASP-10 (1.5Å). HIF1A could bind to quercetin by hydrogen bonds with GLN-369 (2.7Å) and ASP-325 (2.3Å). HIF1A was docked to stigmasterol by hydrogen bond with ASN-283 (1.9Å). TP53 could bind to isorhamnetin with four hydrogen bonds, including THR-170 (2.8Å), VAL-172 (2.4Å), ARG-174 (2.0Å) and HIS-214 (1.9Å). AKT1 was docked to isorhamnetin by hydrogen bonds with GLN-104 (2.3Å) and GLN-61 (1.8Å). JUN could bind to kaempferol with two hydrogen bonds, including DT-36 (2.7Å) and DA-35 (2.4Å). CASP3 was docked to isorhamnetin by hydrogen bonds with LYS-271 (2.4Å), SER-36 (2.3Å), LYS-38 (1.8Å) and GLY-153 (1.8Å). EGFR could bind to beta-sitosterol with ARG-776 (2.4Å) and LEU-778 (1.8Å). Visualization by PyMOL 3.0.4 of molecular docking patterns of key components and key targets of CHDGT in the treatment of BC (Figure 3).

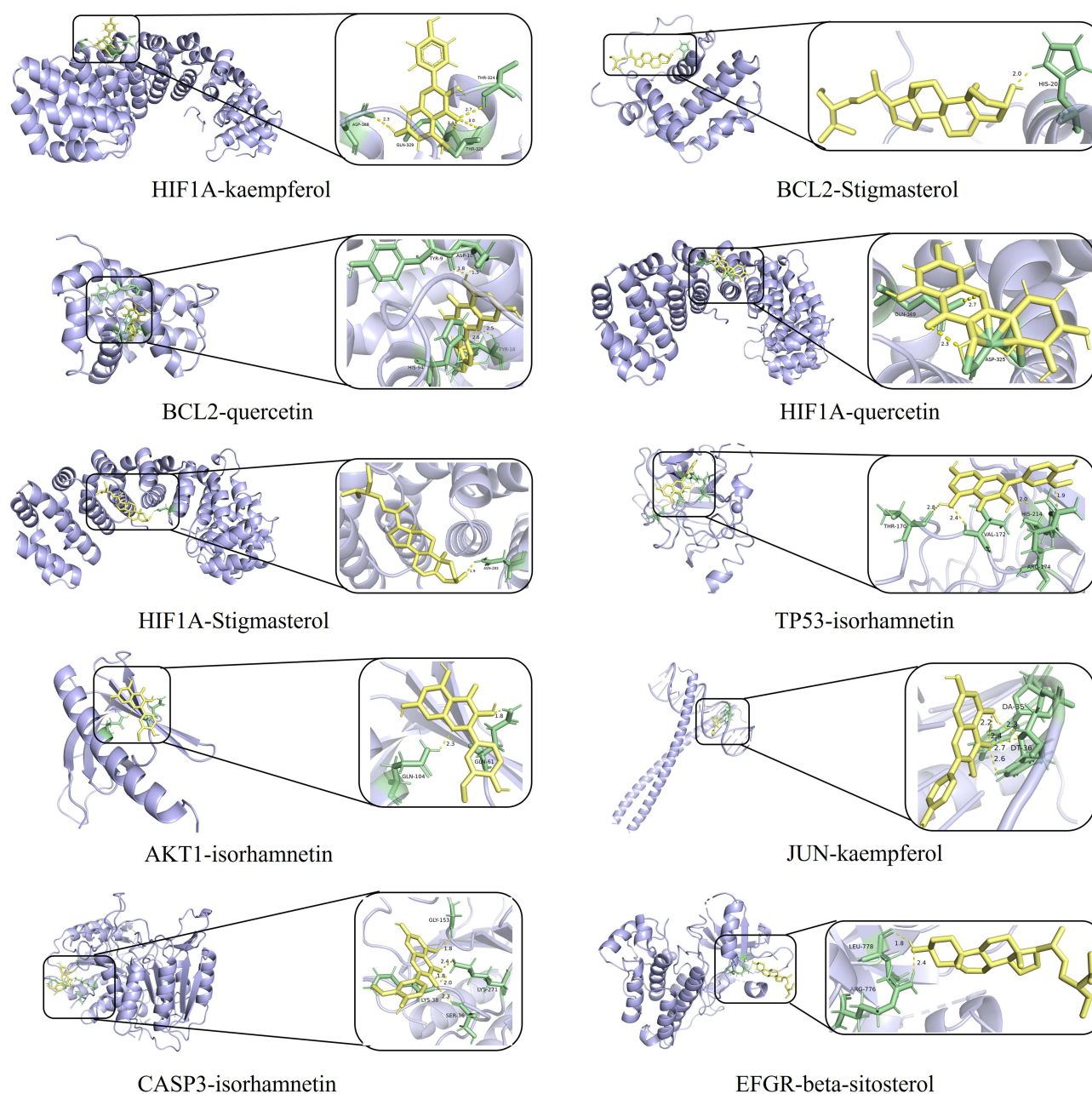


Figure 3 The results of molecular docking analysis of key components and the core targets.

In vitro Cytotoxicity of CHDGT

To assess the effect of CHDGT on 4T1 cells, CCK-8 assay was used to measure cell viability after incubation with different concentrations of CHDGT (0, 50, 100, and 150 mg L⁻¹) at different times (24, 48, and 72 hours). The results showed a dose- and time-dependent inhibitory effect on 4T1 cell proliferation (Figure 4A–C). The IC₅₀ values for 4T1 cells were 201.3 mg L⁻¹ at 24 h and 102.9 mg L⁻¹ at 48 h, and 43.74 mg L⁻¹ at 72 h. Increased incubation time correlated with enhanced cytotoxicity, and at 100 mg L⁻¹ after 48 hours, the cell inhibition rate reached approximately 50%.

Promotion of Apoptosis in 4T1 Cells by CHDGT

Apoptosis is a kind of spontaneous and orderly cell death controlled by genes, involving the activation, expression and regulation of a series of genes.¹¹ Annexin V-FITC/PI staining and flow cytometry were used to observe the effect of CHDGT on apoptosis of 4T1 cells. Additionally, the expression of apoptosis-related genes was examined through qRT-PCR analysis. The apoptosis rate in CHDGT-treated 4T1 cells (100 mg L⁻¹ for 48 hours) reached 50.96 ± 8.51%, significantly higher than the control group rate of 3.84 ± 2.31% (Figure 4D). Furthermore, qRT-PCR results revealed upregulation of pro-apoptotic genes (Caspase3 and p53) and downregulation of the anti-apoptotic gene (Bcl-2) (Figure 5A). These results indicated that CHDGT can promote apoptosis in 4T1 cells.

Potential Mechanism of Antitumor Effect of CHDGT

The expression of HIF-1α in the HIF-1 signaling pathway was evaluated using qRT-PCR analysis (Figure 5B). The results showed that compared with the control group, the expression of HIF-1α gene in 4T1 cells treated with different

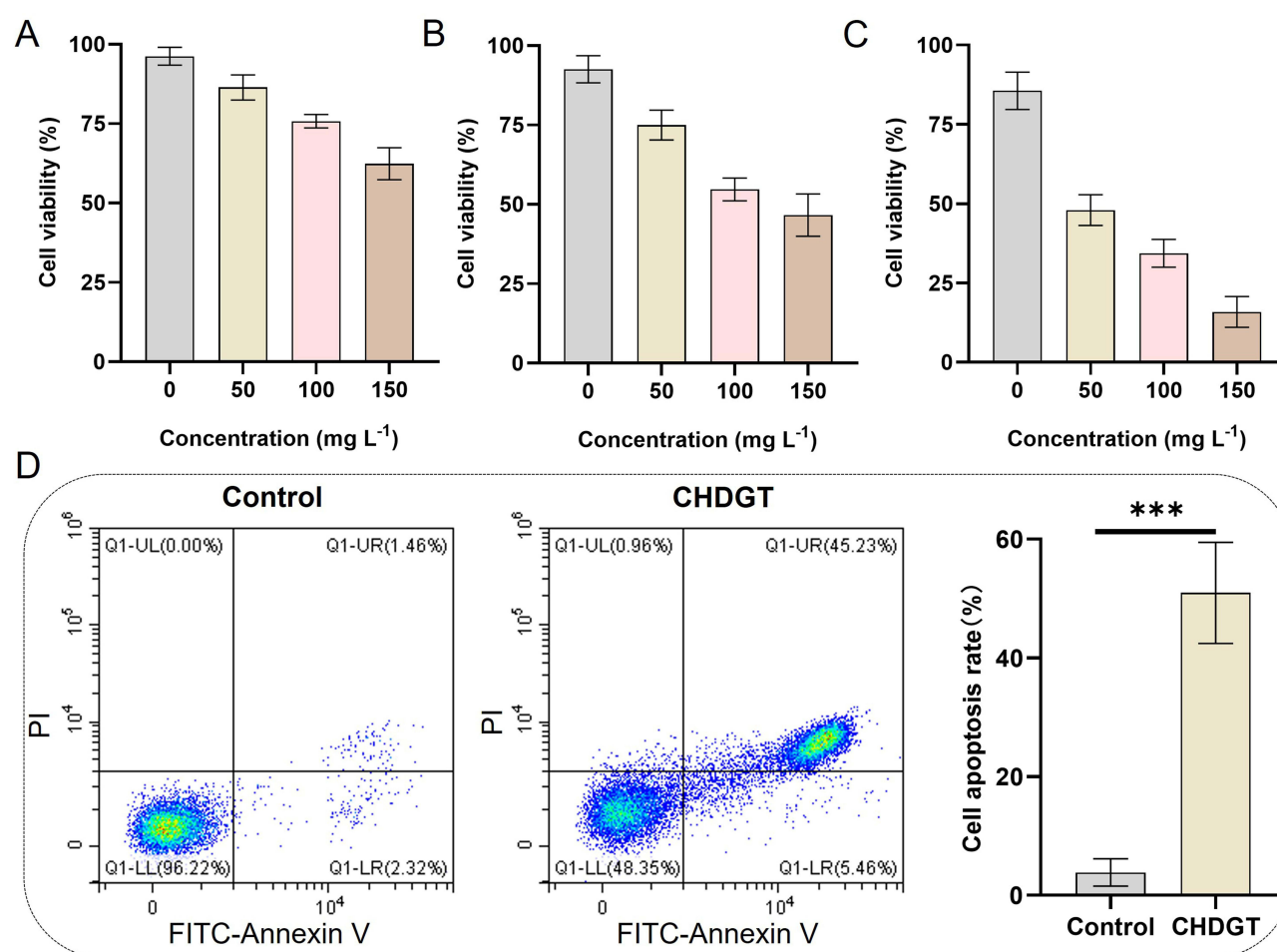


Figure 4 Cytotoxicity of 4T1 cells incubated with the CHDGT: (A) 24 h, (B) 48 h, and (C) 72 h. (D) Analysis of the apoptosis of 4T1 cells. *** P < 0.001.

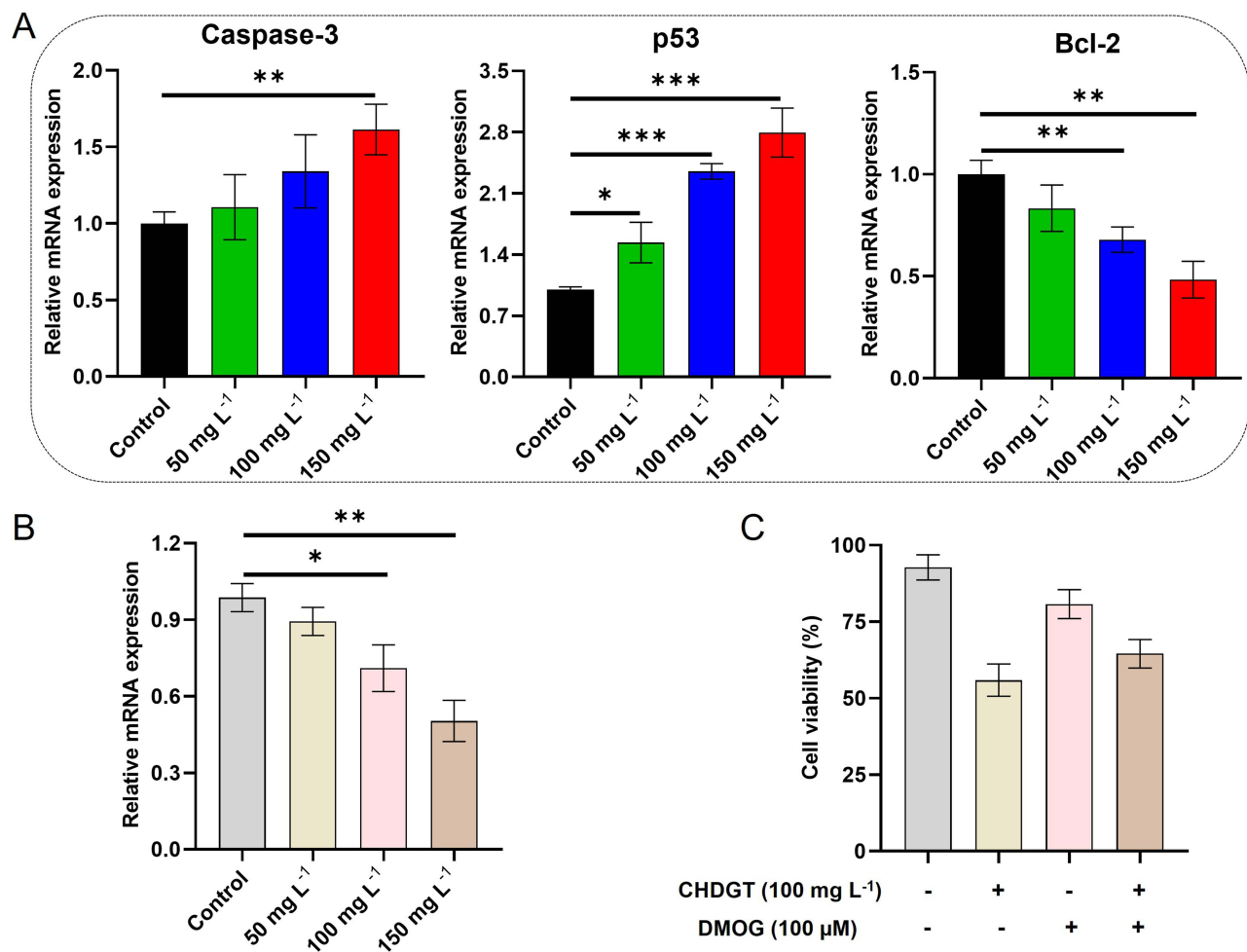


Figure 5 Level of gene expression in CHDGT-incubated 4T1 cells: (A) Caspase-3, p53 and Bcl-2, and (B) HIF-1α. (C) Effects of CHDGT and DMOG on the viability of 4T1 cells. ***P < 0.001, **P < 0.01, and *P < 0.05.

concentrations of CHDGT for 48 h was significantly decreased. Moreover, the addition of HIF-1 pathway activator (DMOG) promoted the proliferation of 4T1 cells (Figure 5C). These suggests that CHDGT exerts its antitumor effects, at least in part, through the modulation of the HIF-1 signaling pathway.

CHDGT Can Inhibit the Growth of BC in vivo

The antitumor effect of CHDGT in vivo was further studied using a mouse model of subcutaneous tumor. When the tumor volume of mice reaches 100 mm³, CHDGT was administered by gavage every three days for 30 days. The tumor growth rate was significantly inhibited in the medium-dose (CHDGT-M, 7 g/kg) and high-dose (CHDGT-H, 14 g/kg) groups compared to the control group (Figure 6A). Calculations of tumor inhibition rates based on tumor volume revealed rates of 27.36 ± 4.38%, 39.31 ± 4.69%, and 60.06 ± 4.82% in the CHDGT-L, CHDGT-M, and CHDGT-H groups, respectively (Figure 6B). The mice were sacrificed 3 days after the last gavage, and tumor tissues were collected and weighed. Tumor weight was significantly reduced in the CHDGT-M and CHDGT-H groups compared to the control group (Figure 6D). Importantly, no significant differences in body weight were observed between groups throughout the treatment period, indicating no observable systemic side effects from CHDGT (Figure 6C). These results confirmed the efficacy of CHDGT in inhibiting BC cell growth.

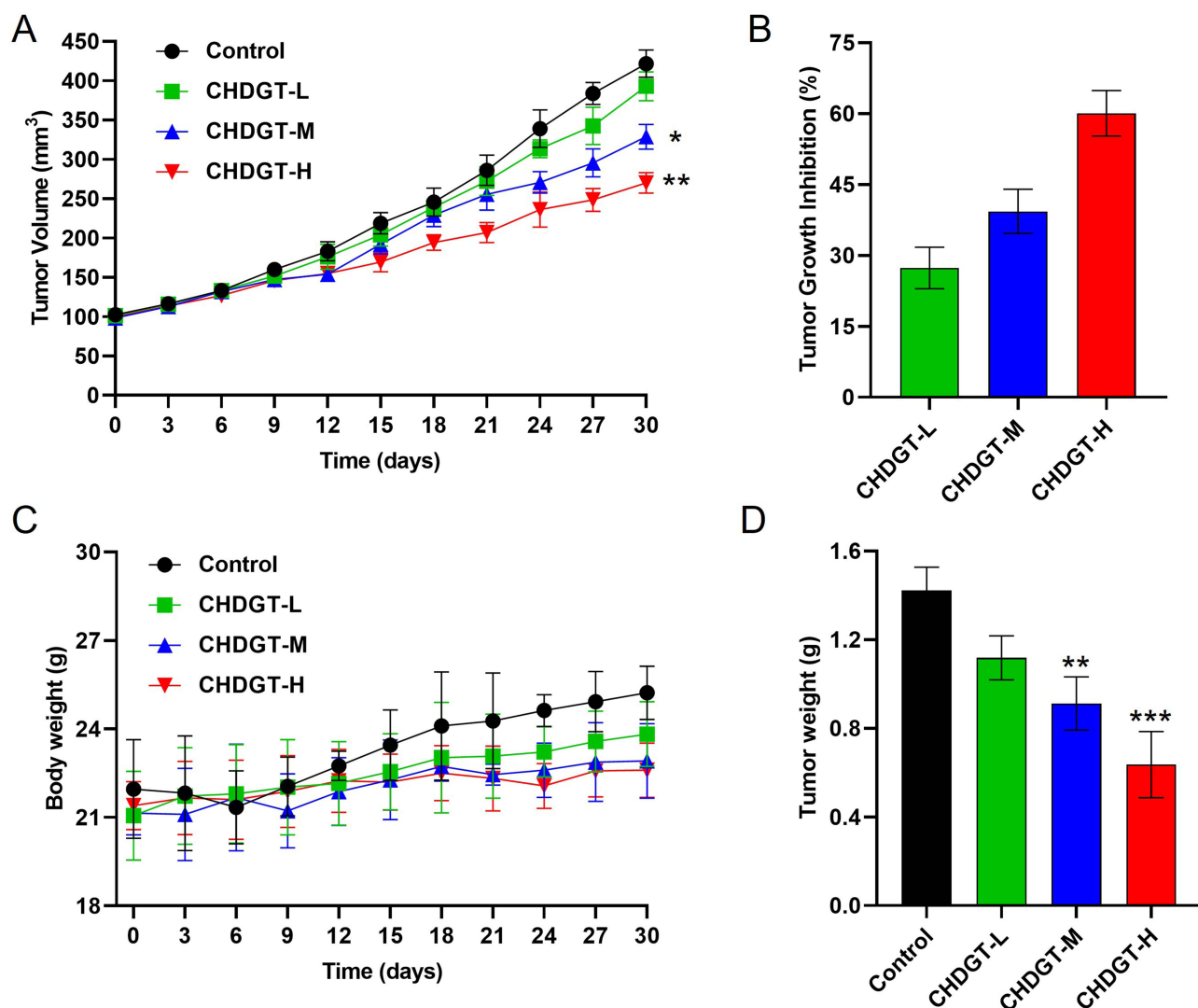


Figure 6 In vivo antitumor efficacy of CHDGT. (A) Tumor volume of mice (n = 6). (B) Tumor inhibition rate (n = 6). (C) Body weight changes (n = 6). (D) The weight of tumor (n = 6). ***P < 0.001, **P < 0.01, and *P < 0.05.

Biosafety and Toxicity in vivo

H&E staining showed no pathological changes in major organs (heart, liver, spleen, lung and kidney) of the mice in different treatment groups, which demonstrated that CHDGT is not toxic at the organ level (Figure 7A). Additionally, the serum was collected and the levels of ALT, AST, ALP, LDH, CRE, and UREA were detected to evaluate in vivo toxicity. The results showed that blood biochemical levels were within the normal range compared to the control group, indicating that liver and kidney function were not impaired (Figure 7B). Therefore, these toxicity studies demonstrate that CHDGT has good biocompatibility and is an effective and safe medicine for cancer therapy.

Discussion

Current therapeutic strategies for breast cancer (BC) primarily involve a multimodal approach that includes surgical resection, radiotherapy, and systemic chemotherapy. Nevertheless, the rates of recurrence and metastasis remain significantly high despite these interventions.¹² Traditional Chinese Medicine (TCM), with its extensive history in managing complex diseases such as severe infections, cardiovascular disorders, and malignancies, has demonstrated promising therapeutic potential.¹³ The unique features of TCM include its diverse bioactive compounds, multi-target mechanisms, and synergistic interactions. Emerging evidence suggests that TCM may exert therapeutic effects in BC

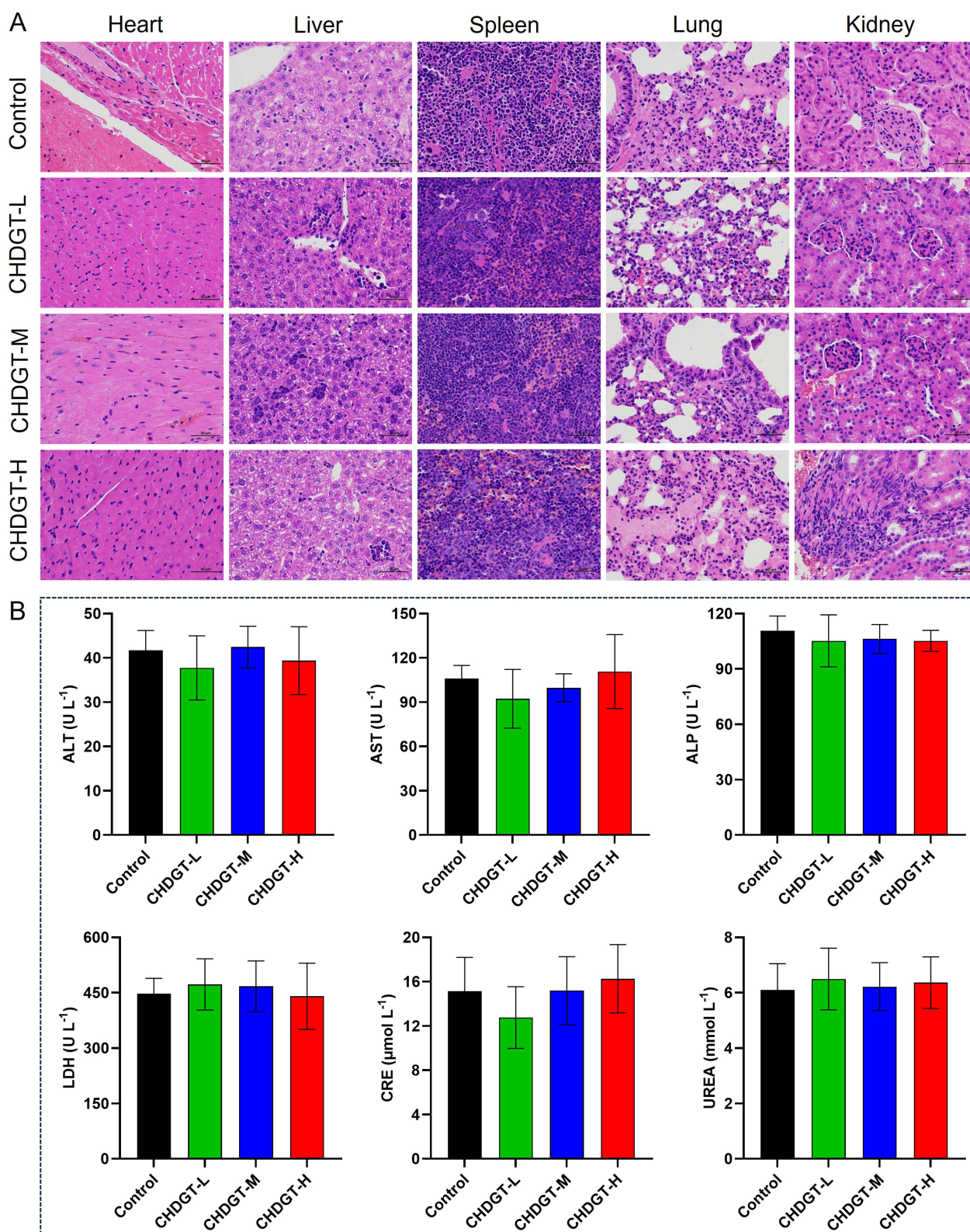


Figure 7 Biosafety and toxicity in vivo. **(A)** Histological evaluation of toxicity of CHDGT. **(B)** Evaluation of serum biochemistry after different treatments.

through mechanisms such as promoting apoptosis and autophagy, suppressing tumor cell proliferation, modulating tumor metabolism, inhibiting epithelial-mesenchymal transition and angiogenesis, and regulating tumor immunity.^{14–16}

CHDGT is a combination of two Chinese herbs, Chaihu and Danggui. Clinical studies have reported its efficacy against various tumors; however, the underlying mechanisms of CHDGT in BC treatment remain unclear. In this study, network pharmacology and molecular docking analyses were employed for the first time to identify the key components, core targets, and potential mechanisms of CHDGT in BC therapy. The anticancer effects of CHDGT were subsequently validated *in vitro* using the mouse breast cancer cell line (4T1). Further, we demonstrated the efficacy of CHDGT in inhibiting BC progression *in vivo* using a 4T1 subcutaneous tumor mouse model. The changes of gene expression in 4T1 cells of control and CHDGT treatment group were analyzed by qRT-PCR, and the potential molecular mechanism of CHDGT in the treatment of BC was investigated by flow cytometry. Finally, we evaluated the blood biochemical index, and organ toxicity through H&E staining.

In this study, the active components of each herb in CHDGT were identified, and a total of 190 drug-related targets were retrieved from relevant databases. Additionally, 1137 BC-associated targets were identified from the GeneCards database. By intersecting the drug targets with the BC targets, 98 overlapping targets were identified. Analysis of the “CHDGT-active ingredients-targets” network revealed that quercetin, stigmasterol, kaempferol, beta-sitosterol, and isorhamnetin had the highest number of BC-related therapeutic targets, suggesting that these ingredients may represent the core bioactive ingredients of CHDGT in BC treatment. Many studies have shown that these active ingredients exert antitumor effects by inducing apoptosis, inhibiting tumor metastasis and invasion, promoting autophagy, blocking cell cycle, inhibiting angiogenesis and antitumor immune activation.^{17–23}

In the PPI network, we identified 8 key genes (TP53, AKT1, JUN, ESR1, BCL2, CASP3, HIF1A, and EGFR), which may be the core targets of CHDGT treatment of BC. TP53 is a critical tumor suppressor gene and regulator of DNA replication, which exerts anti-tumor effects by inducing apoptosis.²⁴ AKT1 regulates the proliferation, survival, and metabolism of tumor cells through pathways related to inflammatory and metabolic processes.²⁵ JUN is involved in a variety of cellular activities, including proliferation, apoptosis, survival, tumorigenesis, and tissue morphogenesis.²⁶ ESR1 (estrogen receptor 1) mutations are associated with tumor progression and metastasis.²⁷ As a key regulator of apoptosis, overexpression of BCL2 has often been observed in a variety of cancers, and its anti-apoptotic effect is closely related to its expression level.²⁸ CASP3 (caspase-3) is indispensable for executing hallmark features of apoptosis, including cell membrane rupture and apoptotic body formation.²⁹ HIF-1 α is a transcriptional activator that depends on oxygen levels. Its upregulation promotes tumor growth via mechanisms such as metabolic reprogramming, angiogenesis, invasion, stem cell maintenance, metastasis, genomic instability, and therapy resistance.³⁰ EGFR (epidermal growth factor receptor) is highly or abnormally expressed in solid tumors and contributes to angiogenesis, tumor cell proliferation, metastasis, invasion, and the inhibition of apoptosis.³¹ In this study, 5 core compounds (quercetin, stigmasterol, kaempferol, beta-sitosterol, and isorhamnetin) were selected for molecular docking verification with the top 8 key targets (TP53, AKT1, JUN, ESR1, BCL2, CASP3, HIF1A, and EGFR), and the results showed that all compounds had good binding ability. These suggesting that CHDGT could inhibit BC progression by targeting these key genes.

GO analysis revealed that CHDGT may exert therapeutic effects on BC by modulating biological processes such as hormonal responses, regulation of apoptotic signaling pathways, positive regulation of programmed cell death, promotion of cell migration, and cell population proliferation. KEGG enrichment analysis identified key pathways potentially involved in CHDGT's mechanisms of action, including HIF-1 signaling pathway, chemical carcinogenesis-reactive oxygen species, FoxO signaling pathway, and necroptosis signaling pathway.

The cell experimental validation supported these predictions, demonstrating that CHDGT inhibits breast cancer cell proliferation, induces apoptosis, and regulates the HIF-1 signaling pathway. These findings align with prior studies on the anti-tumor properties of CHDGT's active ingredients, underscoring the potential of TCM in contemporary cancer therapy. The results of CCK-8 assays, flow cytometry, and qRT-PCR suggest that CHDGT exhibits cytostatic and cytotoxic effects against BC cells. A pivotal discovery of this study is the involvement of the HIF-1 signaling pathway in CHDGT's anti-breast cancer activity. The HIF-1 pathway plays an important role in tumor adaptation to hypoxia and is critically associated with cancer progression, invasion, metastasis, and resistance to therapy.³² Notably, CHDGT treatment was associated with significant downregulation of HIF-1 α gene expression, suggesting a mechanism involving HIF-1 α degradation and subsequent

inhibition of the HIF-1 pathway. Further, activation of the HIF-1 pathway using DMOG enhanced the proliferation of 4T1 cells, corroborating the role of HIF-1 α in BC progression. Shi et al previously reported that HIF-1 α expression is particularly elevated in breast cancer cells, and its inhibition can deactivate Bcl-2, initiate caspase cascades, and induce apoptosis.³³ Additionally, active ingredients in CHDGT, such as quercetin and kaempferol, have been shown to prevent the accumulation of HIF-1 α under hypoxic conditions.^{34,35} The animal experiments further confirmed that CHDGT can effectively inhibit the progression of BC cells, and has good biocompatibility, which is an effective and safe cancer treatment drug.

The aim of this study is to investigate the efficacy and mechanism of CHDGT in the treatment of BC. The key findings and contributions of this study include the following: (1) The key ingredients, core targets, and signaling pathways of CHDGT in the treatment of BC were analyzed by network pharmacology. (2) The good binding ability of key ingredients to core targets was verified by molecular docking. (3) CHDGT inhibited BC cell proliferation in a time- and dose-dependent manner while promoting BC cell apoptosis through in vitro experiments. (4) Animal experiments verified that CHDGT can significantly inhibit the progression of BC without organ toxicity. (5) In addition, CHDGT may exert anti-BC effects by regulating HIF-1 signaling pathway. Despite the promising findings, several limitations should be acknowledged. Although we have demonstrated the anticancer effect of CHDGT on BC, the mechanism by which CHDGT inhibits BC is not fully enough. Therefore, in future studies, we will further explore the main active ingredients and more detailed mechanisms of CHDGT inhibiting BC.

Conclusion

Our research confirmed antitumor efficacy of CHDGT and studied its key ingredients, core targets, and possible mechanism by network pharmacology, molecular docking, and experiments. These findings suggest that CHDGT acts through multiple targets and pathways related to BC, in line with the holistic principles of TCM. In vitro, the results of CCK-8 assay showed that CHDGT can dose-dependently inhibits BC cell growth, and at 100 mg L⁻¹ after 48 hours, the cell inhibition rate reached approximately 50%. Further analysis showed that CHDGT can promote apoptosis of BC cell, and regulate the expression levels of apoptosis-related genes, such as Caspase3, p53, and Bcl-2. The animal experiments verified that CHDGT can significantly inhibit the progression of BC, the tumor inhibition rate of CHDGT-H groups was as high as 60.06 \pm 4.82%. In addition, H&E staining and blood biochemical analysis suggest that CHDGT exhibits favorable safety. This study may provide perspectives for the development of anticancer Chinese herbs for the treatment of BC. However, the main active ingredients and more detailed mechanisms of CHDGT inhibition on BC still need to be further explored in future studies.

Abbreviations

TCM, traditional Chinese medicine; BC, breast cancer; JUN, Jun Proto-Oncogene; OB, oral bioavailability; ESR1, Estrogen Receptor 1; DL, drug-likeness; BCL2, BCL2 Apoptosis Regulator; GO, Gene Ontology; AKT1, AKT Serine/Threonine Kinase 1; KEGG, Kyoto Encyclopedia of Genes and Genomes; EGFR, Epidermal Growth Factor Receptor; DMEM, Dulbecco's modified Eagle's medium; HIF1A, Hypoxia Inducible Factor 1 Subunit Alpha; CC, cellular component; ALT, alanine aminotransferase; MF, molecular function; AST, aspartate aminotransferase; BP, biological process; ALP, alkaline phosphatase; DMOG, Dimethyloxallyl Glycine; LDH, lactic dehydrogenase; FBS, fetal bovine serum; CRE, serum creatinine; PPI, Protein-protein interaction; UREA, urea nitrogen.

Data Sharing Statement

Data available on request from the authors.

Funding

The work was supported by the National Natural Science Foundation of China (82104629, 8200410), the Natural Science Foundation of Guangdong Province (2021A1515010673, 2023A1515011078), the Natural Science Foundation of Hainan Province (82MS157), Medical Scientific Research Foundation of Guangdong Province, China (A2024727, A2024779), Traditional Chinese Medicine Administration Project of Guangdong Province (20231389, 20221256), Science and Technology Program of Yangjiang (SF2021049, SF2022001, SF2023026, SF2023027), and the Scientific Research Fund of Yangjiang People's Hospital (2021003, G2021002, G2021004).

Disclosure

The authors declare no conflicts of interest in this work.

References

- Bray F, Laversanne M, Sung HYA, et al. Global cancer statistics 2022: GLOBOCAN estimates of incidence and mortality worldwide for 36 cancers in 185 countries. *CA*. 2024;74:229–263. doi:10.3322/caac.21834
- Akram M, Iqbal M, Daniyal M, Khan AU. Awareness and current knowledge of breast cancer. *Biol. Res.* 2017;50:1–23.
- Feng R, Pan L, Yao Y, Gao J, Zhang X. Impact of hormone receptor and HER2 conversions on survival after neoadjuvant chemotherapy in breast cancer patients. *Oncol Trans Med.* 2025;11(2):73–80. doi:10.1097/ot9.0000000000000078
- Zhao ZQ, Zhu YX, Long FY, Ma Y, Tang Q, Wang T. Exploring the potential of Huangqin Tang in breast cancer treatment using network pharmacological analysis and experimental verification. *BMC Complement Med Therap.* 2024;24. doi:10.1186/s12906-024-04523-0
- Wu HB, Xiao YG, Chen JS, Qiu ZK. The potential mechanism of Bupleurum against anxiety was predicted by network pharmacology study and molecular docking. *Metab Brain Dis.* 2022;37:1609–1639. doi:10.1007/s11011-022-00970-1
- Wei WL, Zeng R, Gu CM, Qu Y, Huang LF. Angelica sinensis in China-A review of botanical profile, ethnopharmacology, phytochemistry and chemical analysis. *J Ethnopharmacol.* 2016;190:116–141. doi:10.1016/j.jep.2016.05.023
- Bi SJ, Huang YX, Feng LM, et al. Network pharmacology-based study on immunomodulatory mechanism of danggui-yimucao herb pair for the treatment of RU486-induced abortion. *J Ethnopharmacol.* 2022;282:114609. doi:10.1016/j.jep.2021.114609
- Lu S, Sun XB, Zhou ZB, et al. Mechanism of Bazhen decoction in the treatment of colorectal cancer based on network pharmacology, molecular docking, and experimental validation. *Front Immunol.* 2023;14. doi:10.3389/fimmu.2023.1235575
- Shang LR, Wang YC, Li JX, et al. Mechanism of Sijunzi Decoction in the treatment of colorectal cancer based on network pharmacology and experimental validation. *J Ethnopharmacol.* 2023;302:115876. doi:10.1016/j.jep.2022.115876
- Ru JL, Li P, Wang JN, et al. TCMSP: a database of systems pharmacology for drug discovery from herbal medicines. *J Cheminf.* 2014;6. doi:10.1186/1758-2946-6-13
- Zhang J, Yin X, Li C, et al. A Multifunctional Photoacoustic/Fluorescence dual-mode-imaging gold-based theranostic nanoformulation without external laser limitations. *Adv Mater.* 2022;34:e2110690. doi:10.1002/adma.202110690
- Kong X, Song J, Gao P, et al. Revolutionizing the battle against locally advanced breast cancer: a comprehensive insight into neoadjuvant radiotherapy. *Med Res Rev.* 2024;44:606–631. doi:10.1002/med.21998
- Lin X, Yang X, Yang Y, Zhang H, Huang X. Research progress of traditional Chinese medicine as sensitizer in reversing chemoresistance of colorectal cancer. *Front Oncol.* 2023;13:1132141. doi:10.3389/fonc.2023.1132141
- Yuan J, Liu Y, Zhang T, et al. Traditional Chinese medicine for breast cancer treatment: a bibliometric and visualization analysis. *Pharm Biol.* 2024;62:499–512. doi:10.1080/13880209.2024.2359105
- Zhou Y, Gong J, Deng X, et al. Curcumin and nanodelivery systems: new directions for targeted therapy and diagnosis of breast cancer. *Biomed Pharmacother.* 2024;180:117404. doi:10.1016/j.biopha.2024.117404
- Yu Q, Xu C, Song J, Jin Y, Gao X. Mechanisms of traditional Chinese medicine/natural medicine in HR-positive breast cancer: a comprehensive literature review. *J Ethnopharmacol.* 2024;319:117322. doi:10.1016/j.jep.2023.117322
- Reyes-Farias M, Carrasco-Pozo C. The anti-cancer effect of quercetin: molecular implications in cancer metabolism. *Int J Mol Sci.* 2019;20:3177. doi:10.3390/ijms2013177
- Sethi G, Rath P, Chauhan A, et al. Apoptotic mechanisms of quercetin in liver cancer. *Recent Trends Adv. Pharm.* 2023;15:712.
- Zhang J, Shen L, Li X, Song W, Liu Y, Huang L. Nanoformulated codelivery of quercetin and alantolactone promotes an antitumor response through synergistic immunogenic cell death for microsatellite-stable colorectal cancer. *ACS Nano.* 2019;13:12511–12524. doi:10.1021/acsnano.9b02875
- Imran M, Salehi B, Sharifi-Rad J, et al. Kaempferol: a key emphasis to its anticancer potential. *Molecules.* 2019;24(12):2277. doi:10.3390/molecules24122277
- Gong G, Guan YY, Zhang ZL, et al. Isorhamnetin: a review of pharmacological effects. *Biomed Pharmacother.* 2020;128:110301. doi:10.1016/j.biopha.2020.110301
- Zhang X, Wang J, Zhu L, et al. Advances in Stigmasterol on its anti-tumor effect and mechanism of action. *Front Oncol.* 2022;12:1101289. doi:10.3389/fonc.2022.1101289
- Bao X, Zhang Y, Zhang H, Xia L. Molecular mechanism of β -sitosterol and its derivatives in tumor progression. *Front Oncol.* 2022;12:926975. doi:10.3389/fonc.2022.926975
- Zhang J, Li C, Xue Q, et al. An efficient carbon-based drug delivery system for cancer therapy through the nucleus targeting and mitochondria mediated apoptotic pathway. *Small Methods.* 2021;5:e2100539. doi:10.1002/smt.202100539
- Li D, Wang G, Jin G, et al. Resveratrol suppresses colon cancer growth by targeting the AKT/STAT3 signaling pathway. *Int J Mol Med.* 2019;43:630–640. doi:10.3892/ijmm.2018.3969
- Meng Q, Xia Y. c-Jun, at the crossroad of the signaling network, Protein Cell. *Protein Cell* 2011;2:889–898.
- Dustin D, Gu G, Fuqua SAW. ESR1 mutations in breast cancer. *Cancer.* 2019;125:3714–3728. doi:10.1002/cncr.32345
- D'Aguanno S, Brignone M, Scalera S, et al. Bcl-2 dependent modulation of hippo pathway in cancer cells. *Cell Commun Signal.* 2024;22:277. doi:10.1186/s12964-024-01647-1
- Eskandari E, Eaves CJ. Paradoxical roles of caspase-3 in regulating cell survival, proliferation, and tumorigenesis. *J Cell Biol.* 2022;221. doi:10.1083/jcb.202201159
- Rashid M, Zadeh LR, Baradaran B, et al. Up-down regulation of HIF-1 α in cancer progression. *Gene.* 2021;798:145796. doi:10.1016/j.gene.2021.145796
- Wang F, Fu X, Chen P, et al. SPSB1-mediated HnRNP A1 ubiquitylation regulates alternative splicing and cell migration in EGF signaling. *Cell Res.* 2017;27:540–558. doi:10.1038/cr.2017.7
- Semenza GL. Targeting HIF-1 for cancer therapy. *Nat Rev Cancer.* 2003;3:721–732. doi:10.1038/nrc1187

33. Shi Y, Chang M, Wang F, Ouyang X, Jia Y, Du H. Role and mechanism of hypoxia-inducible factor-1 in cell growth and apoptosis of breast cancer cell line MDA-MB-231 *Oncol Lett.* **2010**;1:657–662.
34. Feitelson MA, Arzumanyan A, Kulathinal RJ, et al. Sustained proliferation in cancer: mechanisms and novel therapeutic targets. *Semin Cancer Biol.* **2015**;35:S25–s54. doi:10.1016/j.semcancer.2015.02.006
35. Akiyama M, Mizokami T, Miyamoto S, Ikeda Y. Kaempferol increases intracellular ATP content in C(2)C(12) myotubes under hypoxic conditions by suppressing the HIF-1 α stabilization and/or by enhancing the mitochondrial complex IV activity. *J Nutr Biochem.* **2022**;103:108949. doi:10.1016/j.jnutbio.2022.108949

Breast Cancer: Targets and Therapy

Publish your work in this journal

Breast Cancer - Targets and Therapy is an international, peer-reviewed open access journal focusing on breast cancer research, identification of therapeutic targets and the optimal use of preventative and integrated treatment interventions to achieve improved outcomes, enhanced survival and quality of life for the cancer patient. The manuscript management system is completely online and includes a very quick and fair peer-review system, which is all easy to use. Visit <http://www.dovepress.com/testimonials.php> to read real quotes from published authors.

Submit your manuscript here: <https://www.dovepress.com/breast-cancer—targets-and-therapy-journal>

Dovepress
Taylor & Francis Group